

First-Principles Calculation of Be(0001) Thin Films: Quantum Size Effect and Adsorption of Atomic Hydrogen

Ping Zhang, Hong-Zhou Song

Institute of Applied Physics and Computational Mathematics, P.O. Box 8009, Beijing 100088, P.R. China

We have carried out first-principles calculations of Be(0001) thin films to study the oscillatory quantum size effects exhibited in the surface energy, work function, and binding energy of the atomic hydrogen monolayer adsorption. The prominent enhancement of the surface density of states at the Fermi level makes Be(0001) thin films more metallic compared to the crystalline Be. As a result, the calculated energetics of Be films and the properties of atomic H adsorption onto Be(0001) surface are featured by a quantum oscillatory behavior. Furthermore, The prominent change in the Be(0001) surface electronic structure by the atomic hydrogen adsorption has also been shown.

PACS numbers: 73.61.-r, 73.20.At, 73.21.Ac,

I. INTRODUCTION

When the thickness of thin films approaches the nanoscale, the oscillatory quantum size effects (QSE) associated with electronic confinement and interference will occur^{1,2,3,4} due to the splitting of the energy-level spectrum into subbands normal to the plane of the films. It has been shown that a change in film thickness by just one atomic layer can result in property variations on the order of $1/N$, where N is the thickness of the film in terms of monolayers (ML). The oscillatory QSE have long been clearly observed in ultrathin metal overlayers on metal substrates⁵. Recent systematic experimental and theoretical investigation of the QSE has mainly been focused to Pb films deposited on Si(111)^{6,7,8,9,10,11,12,13,14,15,16,17,18,19,21,22} or Cu(111)²³ substrates.

In this paper we present a detailed first-principles study of the electronic structure and adsorption energetics of Be free standing films. The QSE in other simple-metal films such as Al^{24,25,26}, Mg²⁴, Li²⁷, Rh²⁴, and Pb^{20,28} have been reported in previous references. Although Be is also a simple metal, its electronic structure is profound compared to its close neighbors in the Periodic Table. In particular, the electronic properties of bulk Be are very distinct from those in Be surface. For instance, the electron density of states (DOS) in bulk Be has a very deep minimum at Fermi level (E_F), making this material nearly semiconducting^{29,30} while in the Be(0001) and Be(10 $\bar{1}$ 0) surfaces the DOS at E_F was found to be larger by a factor of 4-5 that makes these surfaces two-dimensional free-electron-like metals³¹. Compared to Mg and Li which have been previously studied^{24,27} in QSE, the bonding energy of Be is surprisingly strong (cohesive energy Be: 3.32 eV/atom, Mg: 1.51 eV/atom, Li: 1.63 eV/atom³²). Also the Debye temperature is very high (Be: 1440 K, Mg: 400 K, Li: 344 K³³). Thus quantum effects should be more pronounced in determining low-temperature structural properties³⁴.

This paper is organized as follows: In Sec. II, the *ab initio* based method and computational details is outlined. In Sec. III, the surface properties of the Be(0001)

films, including the electronic structure, surface energy, work function, and interlayer relaxation, as a function of the thickness of the films, are presented and discussed. Also the properties of adsorption of atomic hydrogen monolayer onto Be(0001) surface is discussed in detail by presenting the sensitivity of the adsorption energy and local DOS to the thickness of the Be(0001) films. Finally, Sec. IV contains a summary of the work and our conclusion.

II. COMPUTATIONAL METHOD

The calculations were carried out using the Vienna *ab initio* simulation package³⁵ based on density-functional theory with ultrasoft pseudopotentials³⁶ and plane waves. In the present film calculations, free-standing Be(0001) films in periodic slab geometries were employed. The periodic slabs are separated by a vacuum region equal to 20 Å. In all the calculations below, a surface (1 × 1) was employed for the supercell slab. The Brillouin-zone integration was performed using Monkhorse-Pack scheme³⁷ with a 11 × 11 × 1 k -point grid, and the plane-wave energy cutoff was set 300 eV. Furthermore, the generalized gradient approximation (GGA) with PW-91 exchange-correlation potential has been employed with all atomic configurations fully relaxed. First the total energy of the bulk hcp Be was calculated to obtain the bulk lattice constants. The calculated a - and c -lattice parameters are 2.272 Å and 3.544 Å, comparable with experimental³⁸ values of 2.285 Å and 3.585 Å, respectively. The use of larger k -point meshes did not alter these values significantly. A Fermi broadening of 0.1 eV was chosen to smear the occupation of the bands around E_F by a finite- T Fermi function and extrapolating to $T = 0$ K.

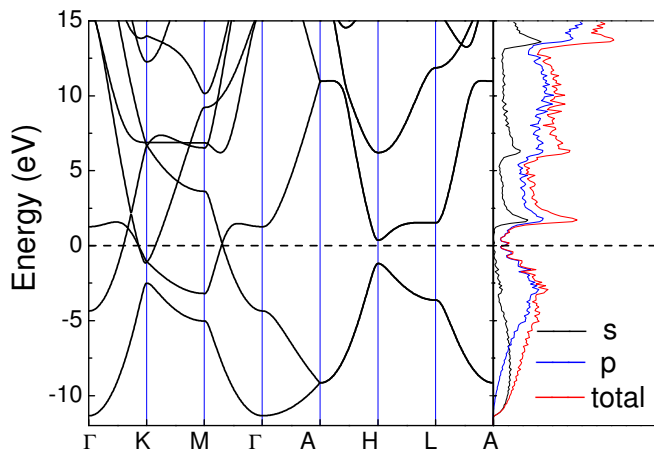


FIG. 1: (Color online) GGA energy bands and density of electron states (right panel) of hcp bulk Be. The dashed line denotes Fermi level.

III. RESULTS AND DISCUSSION

A. Band structure

We first studied the properties of electronic structures of Be(0001) films. As a first step, we present in Fig. 1 the band structure and the DOS of bulk hcp Be. One can see that the density of electronic states for bulk Be resembles somewhat that of a semiconductor since it has a minimum at the Fermi energy. This makes Be different from its close neighbors, such as Mg, whose band property is nearly free-electron like. The bulk Be bands display a direct gap in a large range of the Brillouin zone, unlike Mg. Mg has a filled state at Γ with energy $\simeq 1.3$ eV³⁴, while the corresponding Be state is above the Fermi energy and its band is nearly flat. This band is the source of both the low density of states near the Fermi energy and the high peak above the Fermi energy. Although the electronic configuration of elemental Be is $1s^2 2s^2$, one can see from Fig. 1 that the p -orbital component in bulk Be plays a main role around E_F . The bonding properties of hcp Be is anisotropic, which can be seen by the fact that the c/a ratio (1.56) is one of the most contracted for hcp metals (for Mg, $c/a \simeq 1.62$). Thus out-of-plane neighbors have shorter bonds than in-plane neighbors. Another evidence (not shown here) of this anisotropy is that the contribution of p_x and p_y orbitals to the DOS is different from that of p_z component³⁹.

The above-mentioned "semiconducting" metallic picture for bulk Be are totally changed in the case of Be(0001) surface. To illustrate this change, the electronic structure properties of Be(0001) film of 10 layers are shown in Fig. 2, wherein the left panels give the results for the unrelaxed structure, while the right panels show the relaxed results. For a film with the thickness of 10 layers, it shows in Fig. 2 no prominent difference in electronic structures between relaxed and unrelaxed

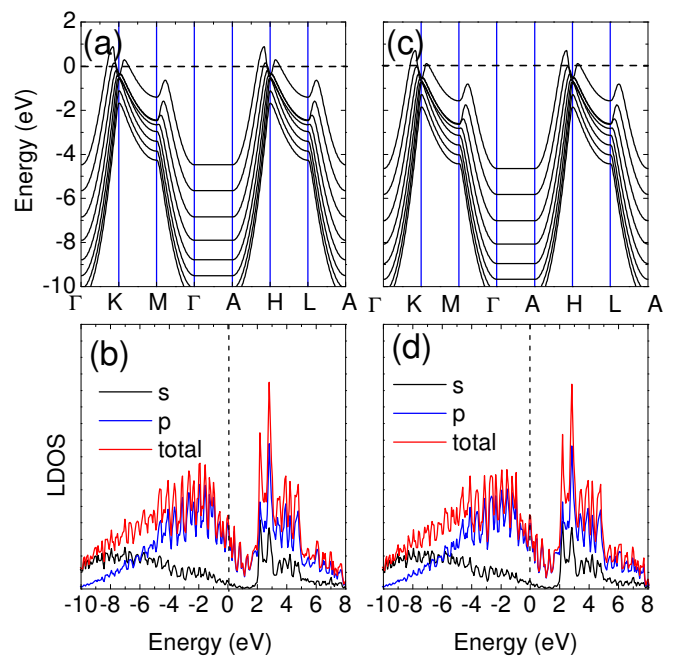


FIG. 2: (Color online) Surface band structures and density of states of a Be(0001) slab with 9 Be monolayers. The left and right panels are for the unrelaxed and relaxed geometries, respectively.

slabs. Compared to the bulk results shown in Fig. 1, it reveals in Fig. 2 that (i) the Fermi level in the Be(0001) film shifts down towards the broad peak, resulting in a prominent enhancement of the DOS at E_F with respect to the bulk case. This phenomenon of high density of surface states at E_F was previously reported³¹, and was also noticed in other metal films such as W(110) and Mo(110)⁴⁰; (ii) the band structure of the Be(0001) slab is characterized by a series of subbands which can be well fit by $E_n + \hbar^2(k_x^2 + k_y^2)/2m^*$ with the effective mass m^* . This clearly demonstrates the quasi-2D free-electron character in the Be(0001) thin film, which is contrary to the bulk Be.

B. Energetics

Figure 3(a) shows the total energy per monolayer $E(N)/N$ as a function of the number N of layers in the slab. The atoms in the slabs have been fully relaxed during the calculations. One can see from Fig. 3(a) that with increasing the thickness, $E(N)/N$ gradually approaches a constant value which in the limit is equal to the energy per atom in the bulk Be.

A quantity more suitably tailored to the QSE is the energy difference $\Delta E(N) = E(N) - E(N - 1)$. This quantity is shown in Fig. 3(b), which reveals damped oscillations as a function of N . These oscillations arise from the occupation of electronic levels close to Fermi

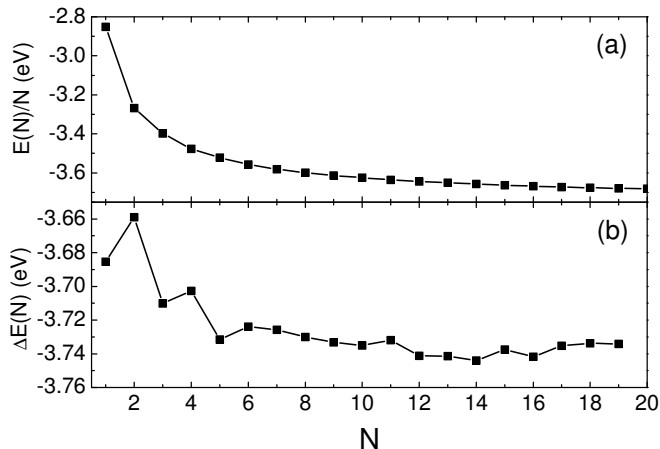


FIG. 3: (a) Monolayer energies $E(N)/N$ for fully relaxed Be(0001) slabs as a function of the number of Be monolayers N ; (b) corresponding energy differences .

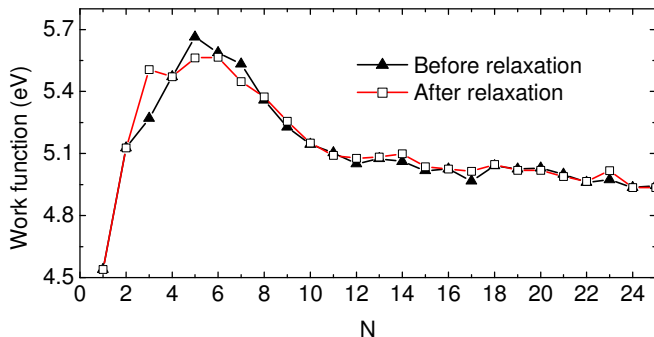


FIG. 4: Work function of Be(0001) thin film as a function of the number of Be monolayers in the slab.

surface⁴¹, which are p -like as shown in Fig. 2.

Figure 4 shows the work function of the Be(0001) thin films as a function of the number of Be layers in the slab for the unrelaxed and the relaxed geometries. One can see that the large influence of the relaxation on the work function occurs in the range of $N \sim 3-7$. For more larger values of N , the overall effect of geometry relaxation on the work function trend is small. Note that unlike the other metals such as Pb(111), in which the work function oscillates periodically even in the ultra-thin film limit, the work function of Be(0001) first curves up at small values of N (~ 3), then lowers down towards the bulk value in an oscillatory way. The peculiar behavior of work function in Fig. 4 implies the more complicated thin-film properties of Be compared to the other simple s - p metals. The similar behavior also occurs in the adsorption energy of atomic hydrogen onto Be(0001) surface (see below).

TABLE I: Interlayer relaxations given in percent, $\Delta d_{i,i+1}$, of Be(0001) as a function of the number N of layers in the slab.

N	Δd_{12}	Δd_{23}	Δd_{34}	Δd_{45}	Δd_{56}	Δd_{67}
2	+10.972					
3	+6.546	+6.546				
4	+5.4	+2.298	+5.4			
5	+3.127	+0.765	+0.765	+3.127		
6	+2.533	-0.181	+0.762	-0.181	+2.533	
7	+2.419	-0.266	+0.062	+0.062	-0.266	+2.419
8	+1.718	-0.767	+0.176	-0.29	+0.175	-0.767
9	+1.5	-0.827	-0.081	+0.052	+0.052	-0.081
10	+1.032	-0.829	-0.001	-0.025	+0.173	-0.025
11	+1.158	-0.920	-0.071	+0.028	+0.092	+0.092
12	+0.935	-1.008	-0.003	-0.214	+0.277	-0.073
13	+1.228	-0.902	-0.09	-0.011	+0.091	+0.031
14	+1.038	-0.951	-0.031	-0.21	+0.216	-0.073
15	+1.228	-1.024	+0.022	-0.225	+0.1789	-0.018

C. Interlayer relaxation

The interlayer relaxation, $\Delta d_{i,i+1}$, are given in percent with respect to the unrelaxed interlayer spacings, d_0 , i.e., $\Delta d_{i,i+1} = 100(d_{i,i+1} - d_0)/d_0$. $d_{i,i+1}$ is the interlayer distance between two adjacent layers parallel to the surface calculated by total energy minimization. $d_0 = c/2$ is the bulk interlayer distance along (0001) direction. As mentioned above, all layers in the slab were allowed to relax. Obviously, the signs + and - of $\Delta d_{i,i+1}$ indicate expansion and contraction of the interlayer spacings, respectively. The relaxation of Be(0001) surface as a function of the number of layers is summarized in Table I. Furthermore, the interlayer relaxations are also plotted in Fig. 5 as a function of N for clear illustration. One can see: (i) The three outmost layers relax significantly from the bulk value, in agreement with experimental observation⁴². In the whole range of layers that we considered, the topmost interlayer relaxation is always outward ($\Delta d_{12} > 0$), with Δd_{12} starting from the largest value of +11% for a slab with only two monolayers, and approaches a final value of $\sim 1\%$ with increasing the thickness of Be(0001) films. Note that the first interlayer separation on most metal surfaces is contracted, Be(0001) is one of the few exceptions. Considering that the calculation is given at zero temperature, our calculated result of $\Delta d_{12} \simeq +1\%$ can be considered comparable with the experimental observation of $\Delta d_{12} \simeq +3\%$ at $T=110$ K. (ii) When the number of monolayers in the slab reaches $N \simeq 5$, the interlayer spacings begin to oscillate with a damped magnitude. Again, the oscillations reflect QSE in Be(0001) thin films. After 25 monolayers, which is the maximal layers considered here, the oscillations are still visible which indicates that the semi-infinite surface limit is still not reached.

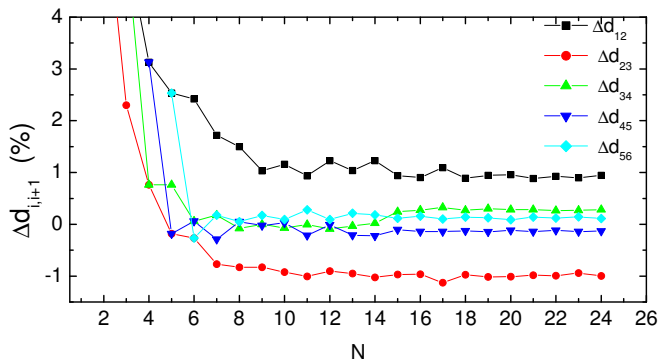


FIG. 5: (Color online) Relaxations of the Be(0001) surfaces as a function of the number N of Be monolayers in the slab

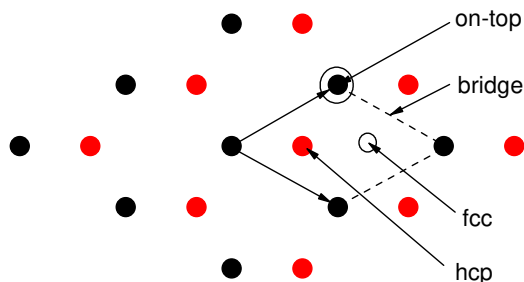


FIG. 6: (Color online) Adsorption sites for H adatoms on the hcp Be(0001) surface. The indicated adsorption sites are on-top, hcp, bridge, and fcc. The H adatoms and Be atoms in the topmost surface layer are indicated by large open circles and small black circles, respectively, while the second-layer Be atoms are depicted as small red circles.

D. Adsorption of atomic hydrogen: QSE of binding energy

To further illustrate the physical properties influenced by finite size of the thin films, in this section we focus our attention to the adsorption of atomic hydrogen on Be(0001) thin films. To the best of our knowledge, the reflection of QSE by the adsorption features has not been previously studied.

Before we study the hydrogen adsorption properties as a function of the thickness of Be(0001) thin films, we need to determine the energetically favourable adsorption site. Since the preference of adsorption site is not sensitive to the thickness of the substrate, thus to look for this preference of the adsorption site, it is sufficient to give a study on the slabs with fixed thickness of the Be(0001) substrate, which at present is chosen to be 9 monolayers. We choose four most probable adsorption sites, namely, on-top, bridge, fcc, and hcp sites, which are indicated in Fig. 6. The binding energy is calculated using the following equation: Binding energy [atomic H] = $-(E[\text{H}/\text{Be}(0001)] - E[\text{Be}(0001)] - 2E[\text{H}])/2$ where $E[\text{H}/\text{Be}(0001)]$ is the total energy of a slab which con-

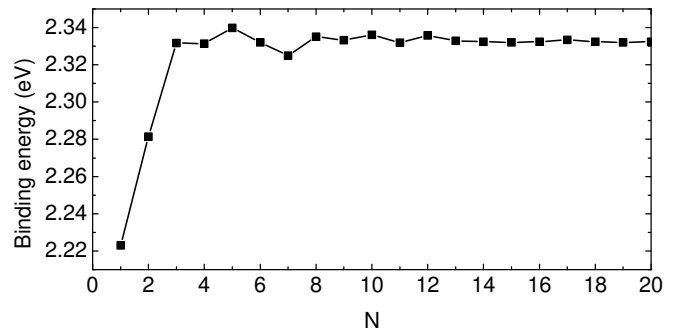


FIG. 7: Calculated binding energy of H adatom as a function the number of Be(0001) monolayers in the slab.

sists of 9 layers of Be atoms and one H atom on each side keeping inversion symmetry, $E[\text{Be}(0001)]$ is total energy of the slab without H atoms, and $E[\text{H}]$ is total energy of a free H atom which is put in a $10 \text{ \AA} \times 10 \text{ \AA} \times 10 \text{ \AA}$ supercell. As a result, the calculated binding energy of atomic H for different adsorption configurations is 1.46 eV (on-top), 2.24 eV (fcc), 2.11 eV (hcp), and 2.33 eV (bridge), showing a clear preference for bridge site adsorption. We note that this bridge-site preference for H adsorption was also reported in Ref.[43] and in other metal surfaces such as W(100)⁴⁴.

After finding the preferred atomic H adsorption site (bridge site), we give a series of calculations for the binding energy of the H adsorbate as a function of the thickness of Be(0001) thin films. The results are summarized in Fig. 7. One can see that the binding energy curves up at small film thickness, followed by damped oscillations when increasing the Be monolayers in the slab. Thus the binding energy of atomic H depends on the thickness of the quantum films in an oscillatory way. In experiment this dependence can be observed by investigating the dependence of H coverage on the monolayers of Be(0001) thin films. Note that the dependence of H adatom binding energy on the thickness of the Be(0001) films looks in analogy with the work function behavior shown in Fig. 4. The cause of this similarity remains unclear at the present stage.

The oscillatory thickness dependence of the binding energy should be related with the bonding properties between H adatom and surface Be atoms. To obtain a deeper understanding of the physics behind this observation, we turn to a full study of the surface electronic structure of H-covered Be(0001). For this we calculate the local density of states (LDOS) through projections of the total wave function onto atoms of interest within the Wigner-Seitz spheres around them. The Wigner-Seitz radii for the H and Be atoms are taken to be 0.5 Å and 1.0 Å, respectively. Figure 8 plots a series of LDOS of H adatom layer and the topmost Be(0001) layer for different thickness of Be thin films. A strong chemical bonding of characteristic molecular H-Be bond can be seen. In the case of ultra-thin slab with only one Be monolayer

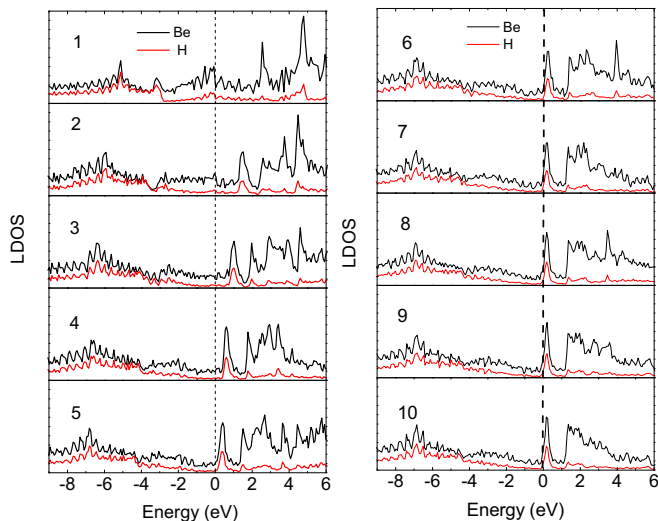


FIG. 8: (Color online) Calculated local density of states of H adatom and topmost Be atom. The number of Be(0001) monolayers in the slabs is shown in the figure.

contained, one can see that the Fermi level falls in the broad-peak region of Be surface. Since the Fermi level for the clean Be(0001) surface also falls in this broad-peak location (see Fig. 2), thus it suggests that adsorption of atomic H onto Be monolayer does not change the surface DOS much. As a consequence, the H binding energy is lowest in the case that only one Be monolayer is included in the slab (see Fig. 7). When the Be(0001) monolayers in the slab is increased, one can see from Fig. 8 that the Fermi energy continuously shifts upwards, approaching a narrow peak, showing a more strong hybridization between H $1s$ and Be $2p$ orbitals. Consequently, the binding energy of H adatom first curves up by increasing the Be layers in the slab, as shown in Fig. 7. When the thickness of slab increases up to 5 Be monolayers, then the Fermi level remains almost unchanged with respect to the narrow peak, the resultant hybridization between H $1s$ and Be $2p$ orbitals obtains its largest amplitude. Therefore, when further increasing the layers of Be in slab, instead of a monotonic increase or decrease, the H adatom bind-

ing energy is now featured by an oscillatory behavior due to metallic nature of Be(0001) surface. Furthermore, by a comparison of the clean-surface DOS (Fig. 2) with the H-adsorbed surface DOS (Fig. 8), remarkably, one can see that there is a prominent change in the Be(0001) surface DOS by the atomic hydrogen adsorption. Since it has been speculated that the metallic enhancement of Be surface is responsible for many extraordinary phenomena such as enhanced electron-phonon coupling⁴⁵, the 400 increase in the superconducting temperature for amorphous Be compared with crystalline Be, clearly it is of high interest to study the effect of H adsorption on these peculiar surface-related phenomena.

IV. CONCLUSION

In summary, the Be(0001) thin films have been studied by density-functional theory pseudopotential plane-wave calculations. The dependence of electronic structure, energetics, and interlayer relaxation upon the thickness of the film has been fully investigated, showing the metallic QSE of the film, although the bulk Be is nearly semi-conducting. We have shown that this QSE is associated with an interplay of surface enhancement at the Fermi level and the bulk band splitting into subbands due to the quasi-2D electronic confinement. We have also studied the atomic hydrogen adsorption onto the Be(0001) films. The results gave a clear preference for bridge site adsorption. We have shown that (i) the H adsorption energy oscillates with increasing the Be monolayers in the slab; (ii) In the case of ultra-thin films, the H adsorbate changes the surface density of states prominently by continuously shifting the Fermi level upwards, approaching the narrow peak in the otherwise clean-surface DOS. The shift will saturate after the thickness of Be(0001) film increases up to 10 layers. We expect this prominent change in the density of states will have a significant effect on the other relevant physical properties in Be(0001) surface.

Acknowledgments

This work was partially supported by the CNSF (Grant No. 10544004 and 10604010).

- ¹ J.J. Paggel, T. Miller, and T.-C. Chiang, *Science* **283**, 1709 (1999).
- ² Z. Tesanovic, M.V. Jaric, and S. Maekawa, *Phys. Rev. Lett.* **57**, 2760 (1986).
- ³ A. E. Meyerovich and S. Stepaniants, *Phys. Rev. Lett.* **73** 316 (1994).
- ⁴ A. Kawabata, *J. Phys. Soc. Jpn.* **62**, 3988 (1993).
- ⁵ T. Miller, A. Samsavar, G.E. Franklin, and T.C. Chiang, *Phys. Rev. Lett.* **61**, 1404 (1988); H. Zeng and G. Vidali, *ibid.* **74**, 582 (1995); B. J. Hinch, C. Koziol, J. P. Toennies, and G. Zhang, *Europhys. Lett.* **10**, 341 (1989).
- ⁶ I. B. Altfeder, D.M. Chen, and K.A. Matveev, *Phys. Rev.*

- Lett.* **80**, 4895 (1998).
- ⁷ V. Yeh, L. Berbil-Bautista, C.Z. Wang, K.M. Ho, and M.C. Tringides, *Phys. Rev. Lett.* **85**, 5158 (2000).
- ⁸ W.B. Su, S.H. Chang, W.B. Jian, C.S. Chang, L.J. Chen, and T.T. Tsong, *Phys. Rev. Lett.* **86**, 5116 (2001).
- ⁹ I.B. Altfeder, V. Narayanamurti, and D.M. Chen, *Phys. Rev. Lett.* **88**, 206801 (2002).
- ¹⁰ P. Czoschke, H. Hong, L. Basile, and T.-C. Chiang, *Phys. Rev. Lett.* **93**, 036103 (2004).
- ¹¹ M.H. Upton, C.M. Wei, M.Y. Chou, T. Miller, and T.-C. Chiang, *Phys. Rev. Lett.* **93**, 026802 (2004).
- ¹² D.A. Ricci, T. Miller, and T.-C. Chiang, *Phys. Rev. Lett.*

- 93**, 136801 (2004).
- ¹³ J.H. Dil, J.W. Kim, S. Gokhale, M. Tallarida, and K. Horn, Phys. Rev. B **70**, 045405 (2004).
- ¹⁴ Y. Guo *et al.*, Science **306**, 1915 (2004).
- ¹⁵ M.H. Upton, T. Miller, and T.-C. Chiang, Phys. Rev. B **71**, 033403 (2005).
- ¹⁶ P. Czoschke, H. Hong, L. Basile, and T.-C. Chiang, Phys. Rev. B **72**, 035305 (2005).
- ¹⁷ P. Czoschke, H. Hong, L. Basile, and T.-C. Chiang, Phys. Rev. B **72**, 075402 (2005).
- ¹⁸ Y.-F. Zhang, J.-F. Jia, T.-Z. Han, Z. Tang, Q.-T. Shen, Y. Guo, Z. Q. Qiu, and Q.-K. Xue, Phys. Rev. Lett. **95**, 096802 (2005).
- ¹⁹ Z.Y. Zhang, Q. Niu, and C. K. Shih, Phys. Rev. Lett. **80**, 5381 (1998).
- ²⁰ C.M. Wei and M.Y. Chou, Phys. Rev. B **66**, 233408 (2002).
- ²¹ Juarez L.F. Da Silva, Phys. Rev. B **71**, 195416 (2005).
- ²² E. Ogando, N. Zabala, E.V. Chulkov, and M.J. Puska, Phys. Rev. B **71**, 205401 (2005).
- ²³ G. Materzanini, P. Saalfrank, and Philip J.D. Lindan, Phys. Rev. B **63**, 235405 (2001).
- ²⁴ P.J. Feibelman, Phys. Rev. B **27**, 1991 (1983); P.J. Feibelman and D.R. Hamann, Phys. Rev. B **29**, 6463 (1984).
- ²⁵ A. Kiejna, J. Peisert, and P. Schraroch, Surf. Sci. **432**, 54 (1999).
- ²⁶ S. Ciraci and I.P. Batra, Phys. Rev. B **33**, 4294 (1985); I.P. Batra, S. Ciraci, G.P. Srivastava, J.S. Nelson, and C.Y. Fong, Phys. Rev. B **34**, 8246 (1986).
- ²⁷ J.C. Boettger and S.B. Trickey, Phys. Rev. B **45**, 1363 (1992); U. Birkenheuer, J.C. Boettger, and N. Rösch, Chem. Phys. Lett. **341**, 103 (1995); K.F. Wojciechowski and H. Bogdanów, Surf. Sci. **397**, 53 (1998); K. Doll, N.M. Harrison, and V.R. Saunders, J. Phys.: Condens. Matter **11**, 5007 (1999).
- ²⁸ P. Saalfrank, Surf. Sci. **274**, 449 (1992).
- ²⁹ D.A. Papaconstantopoulos, *Handbook of Band Structure of Elemental Solids* (Plenum, New York, 1986).
- ³⁰ I. Yu. Sklyadneva, E.V. Chulkov, W.-D. Schöne, V.M. Silkin, R. Keyling, and P.M. Echenique, Phys. Rev. B **71**, 174302 (2005).
- ³¹ E.V. Chulkov, V.M. Silkin, and E.N. Shirykalov, Surf. Sci. **188**, 287 (1987); Ph. Hofmann, R. Stumpf, V.M. Silkin, E.V. Chulkov, and E.W. Plummer, *ibid.* **355**, L278 (1996).
- ³² C. Kittel, *Introduction to Solid State Physics*, 5th ed. (Wiley, New York, 1976).
- ³³ *American Institute of Physics Handbook*, edited by D.E. Gray, 3rd ed. (McGraw-Hill, New York, 1972), Table 4e-10.
- ³⁴ M. Lazzeri, Ph.D. Thesis, Oct. 1999 SISSA, Trieste.
- ³⁵ G. Kresse and J. Furthmüller, Phys. Rev. B **54**, 11169 (1996).
- ³⁶ D. Vanderbilt, Phys. Rev. B **41**, 7892 (1990).
- ³⁷ H.J. Monkhorst and J.D. Pack, Phys. Rev. B **13**, 5188 (1976).
- ³⁸ V.M. Amonenko, V. Ye. Ivanov, G.F. Tikhinskij, and V.A. Finkel, Phys. Met. Metallogr. **14**, 47 (1962).
- ³⁹ M.Y. Chou, Pui K. Lam, and M.L. Cohen, Phys. Rev. B **28**, 4179 (1983).
- ⁴⁰ E. Rotenberg, J. Schaefer, and S.D. Kevan, Phys. Rev. Lett. **84**, 2925 (2000).
- ⁴¹ F.K. Schulte, Surf. Sci. **55**, 427 (1976).
- ⁴² K. Pohl, J.-H. Cho, K. Terakura, M. Scheffler, and E.W. Plummer, Phys. Rev. Lett. **80**, 2853 (1998); H.L. Davis, J.B. Hannon, K.B. Ray, and E.W. Plummer, *ibid.* **68**, 2632 (1992).
- ⁴³ R. Stumpf and P.J. Feibelman, Phys. Rev. B **51**, 13748 (1995).
- ⁴⁴ M.R. Barnes and R.F. Willis, Phys. Rev. Lett. **41**, 1729 (1978).
- ⁴⁵ E.W. Plummer, J. Shi, S.-J. Tang, E. Rotenberg, and S.D. Kevan, Prog. in Surf. Sci. **74**, 251 (2003).
- ⁴⁶ E. Wachowicz and A. Kiejna, J. Phys.: Condens. Matter **13**, 10767 (2001).